SEMARAK ILMU PUBLISHING

Journal of Advanced Research in Fluid Mechanics and Thermal Sciences

Journal homepage:
https://semarakilmu.com.my/journals/index.php/fluid_mechanics_thermal_sciences/index
ISSN: 2289-7879

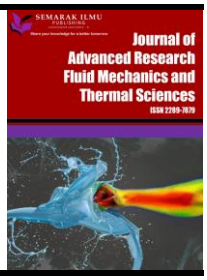

Impact of Magnetohydrodynamics on Hyperbolic and Walters-B Non-Newtonian Fluids

Anumolu Anupama[1], Hari Krishna Yaragani[2], Bojja Ramesh Reddy[3], Tagallamudi Srinivasa Rao[4], Venkata Ramana Reddy Gurrampati[4,*]

[1] Department of Mathematics, DVR & Dr. HS MIC College of Technology, Kanchikacherla, Ponnavaram, Andhra Pradesh 521180, India
[2] Department of H&S, ANURAG Engineering College, Ananthagiri, Kodad, Suryapet, Telangana 508206, India
[3] Department of ECE, Lakireddy Bali Reddy College of Engineering, Mylavaram, 521230, India
[4] Department of Mathematics, Koneru Lakshmaiah Education Foundation, Vaddeswaram, Andhra Pradesh 522302, India

ARTICLE INFO

Article history:
Received 25 September 2023
Received in revised form 12 December 2023
Accepted 26 December 2023
Available online 15 January 2024

Keywords:
Hyperbolic tangent liquid; magnetic field; Walters-B liquid; spectrum relaxation method

ABSTRACT

The current study examines the impact of two non-Newtonian fluids hyperbolic tangent and Walters B fluids transferring heat and mass through an upward-facing, semi-infinite porous plate into the boundary layer. PDEs are used to determine how the flow analysis works. Using the proper similarity functions, the collection of PDEs is condensed into a set of dimensionless ODEs. The spectrum relaxation method (SRM) was used to solve the simplified equations. By initially decoupling the system of coupled equations, SRM solves differential equations repeatedly. The simultaneous flow of two non-Newtonian fluids with flow characteristics including radiation, Soret, viscous dissipation, Joule heating, magnetic field, etc. is elucidated in these communications, which are regarded as being one of a kind. The electrically conductive liquids' flow direction is subjected to a uniformly strong magnetic field.

1. Introduction

The simulation of many manufacturing processes in mechanical engineering and the manufacturing industries heavily relies on the boundary layer flow of non-Newtonian materials. The creation of sticky tape, plastic sheet aerodynamics, cooling, metallic plates, the transfer of coatings and layers onto stiff substrates, and other procedures are a few examples of these manufacturing techniques. Hayat *et al.,* [1], Khan *et al.,* [2,3], and Adnan *et al.,* [4] contain some significant studies on boundary layer flow. Neffah *et al.,* [5], Eberhard *et al.,* [6], Gomez-Constante and Rajagopal [7], Ionescu *et al.,* [8], and Seybold *et al.,* [9] emphasized a few tremendous research works containing non-Newtonian fluid flow through different geometries. Also, the literature presents numerous constitutive equations to analyse the properties of non-Newtonian fluids [10-12]. The model of tangent hyperbolic fluid is sufficient to adequately explain the occurrence of shear thinning. It assesses the fluid's ability to endure a lower flow rate with a higher rate of shear stress. Blood, paint,

* *Corresponding author.*
E-mail address: gvrr1976@kluniversity.in

https://doi.org/10.37934/arfmts.113.1.8294

ketchup, and other liquids are examples of substances that exhibit this feature. Non-uniform heat source/sink and radiation effects on Walter's-B fluid flow past a porous stretching surface are discussed by Hayat *et al.,* [13]. Reddy *et al.,* [14] have studied the entropy generation of a tangent hyperbolic fluid flow past a vertical microchannel with a square density temperature variation. Also, viscous and elastic behaviors are considered in Walters' B fluid model. Hussain and Ullah [15] have discussed the behavior of two different variable viscosity models on the steady-state flow of Walters' B fluid through a stretching cylinder. Tonekaboni *et al.,* [16] have studied the Blasius flow, stagnation-point flow, and Sakiadis flow for viscoelastic Walters' B fluid flows. The stability properties of Walters' B fluid between two rigid cylindrical surfaces are studied by Awasthi *et al.,* [17].

The physical-mathematical framework that deals with the dynamics of magnetic fields in electrically conducting fluids is called magnetohydrodynamics (MHD). In astrophysical plasmas, it is quite significant. MHD pumps, MHD meters, and bearings are other real-world examples. MHD is also very useful in diagnosing diseases, therefore it has uses in bioengineering as well. Researchers looked into MHD's effects on Newtonian and non-Newtonian fluids as a result of its widespread use. The impact of MHD tangent hyperbolic fluid past a stretching sheet in the presence of a convective boundary is studied by Hussain *et al.,* [18]. Ali *et al.,* [19] have examined the effect of MHD on tangent hyperbolic fluid flow past a stretched sheet. Ibrahim [20] has discussed the MHD and radiation effects on tangent hyperbolic nanofluid past a stretching sheet and showed that radiation upturns the thickness of the thermal boundary layer. Usman *et al.,* [21] have investigated the MHD effect on the unsteady state model of tangent hyperbolic fluid and the MLWM method adopted to examine the behavior of the model. The idea of gyrotactic microorganisms and Rosseland approximation in the two-dimensional steady-state flow of Walter's B nanofluid past a stretching sheet is explored by Chu *et al.,* [22]. The impact of Newtonian heating on the MHD boundary layer flow of Walter's B fluid is studied by Hayat *et al.,* [23]. Asjad *et al.,* [24] have developed a mathematical model involving the Caputo Fabrizio time derivative model to examine the effect of MHD on Walter's-B fluid and acquired the results by the Laplace transform method. Salahuddin *et al.,* [25] was investigated the effect of Coriolis and buoyancy forces on three-dimensional flow of chemically reactive tangent hyperbolic fluid subject to variable viscosity. Analysis of tangent hyperbolic nanofluid impinging on a stretching cylinder near the stagnation point was described by Salahuddin *et al.,* [26]. Dharmaiah *et al.,* [27] has analysed the numerical analysis of heat and mass transfer with viscous dissipation, Joule dissipation, and activation energy. Kumar *et al.,* [28] was studied the perturbation methodology for electromagnetic radiative fluxing of chemical reactive Casson fluid flow under heat source (sink) effectiveness Many researchers studied the effects of Cattaneo-Christov heat flux on chemically reacting nanofluids flow past a stretching sheet with joule heating effect and Soret-Dufour mechanisms on unsteady boundary layer flow of tangent hyperbolic flows [29-37].

The core interest of the current work is to examine the MHD effect on the flow and heat transfer of Walters-B and tangent hyperbolic liquids past a semi-infinite porous plate. Soret effect, magnetic field, thermal radiation, and viscous dissipation effects are adopted in this work. The spectrum relaxation method is utilized to solve the governing nonlinear equations. The flow and heat transport characteristics of Walters-B and tangent hyperbolic liquids are discussed for various flow-embedded parameters and portrayed in graphical and tabular forms.

2. Mathematical Formulation

From Figure 1, consider the flow of Walters-B and tangent hyperbolic liquid past a vertical plate inserted into a permeable channel at the same time. The flow regiment is in $y^* > 0$ and the normal in y^* direction. The Walters-B liquids' electrical conductivity and the tangent hyperbolic MHD

property impose a uniform magnetic strength B_0 in a perpendicular direction. A very small magnetic field Reynolds number implies induced magnetic field can be neglected. At rest, the fluid attains same temperature as the plate. An oscillatory time is noticeable in a moment $t < 0$. Furthermore, the impact of thermal radiation alongside the heat source parameter is assumed on the temperature equation. Also, the concentration specie is high such that the impact of Soret and Dufour is not negligible. Using Hussain *et al.,* [18] as a reference and the Cauchy stress tensor definition as follows:

$$T = -pI + S \tag{1}$$

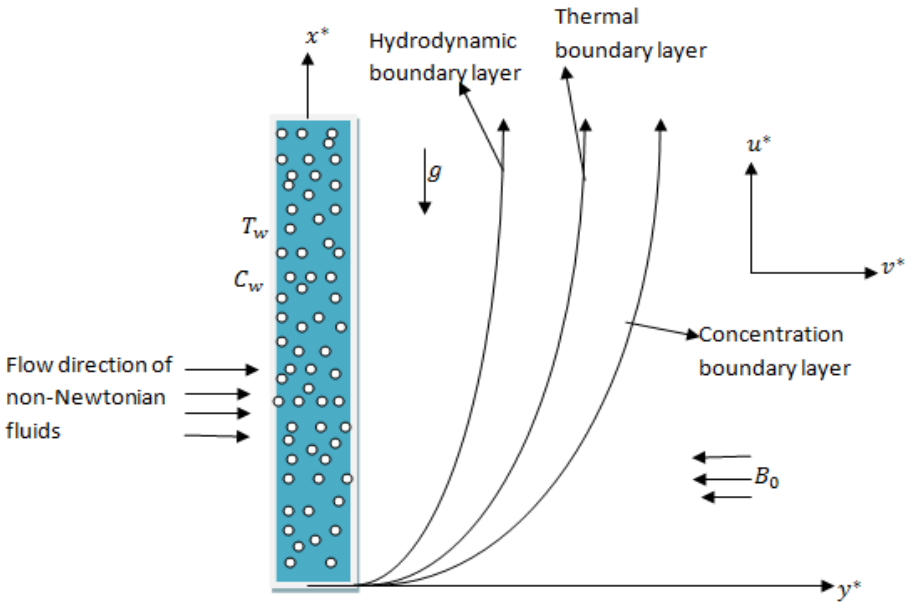

Fig. 1. Physical geometry

Constitutive study of the extra tensor of tangent hyperbolic liquid provides:

$$S = [\mu_\infty + (\mu_0 + \mu_\infty)\tanh(\Gamma\dot{\gamma})^n]A_1 \tag{2}$$

where denotes n-the power law index, Γ the dependent material constant, μ_∞ the shear rate viscosity, μ_0 the zero shear rate viscosity, and A_1 the first tensor Rivlin-Erickson.

From the above, $\dot{\gamma}$ gives:

$$\dot{\gamma} = \sqrt{\frac{1}{2}tr(A_1^2)} \tag{3}$$

For the sake of simplicity, consider $\mu_\infty = 0$ in Eq. (2) and since tangent hyperbolic liquid explains shear thinning analysis. Therefore, $\Gamma \det \gamma < 1$. Utilizing the above simplifications on Eq. (2) to obtain:

$$S = \mu_0[(\Gamma\dot{\gamma})]A_1 \tag{4}$$

Simplifying the above to obtain

$$S = \mu_0[1+n(\Gamma\dot{\gamma}-1)]A_1 \tag{5}$$

The constitutive analysis of the Walters-B liquid is described as follows:

$$\sigma_{ik} = -pg_{ik} + \sigma'_{ik} \tag{6}$$

$$\sigma'^{ik} = a\eta_0 e^{ik} - 2k_0 e'^{ik} \tag{7}$$

where η_0 is the limiting viscosity at small rates of shear, k_0 is the elastic co-efficient, σ^{ik} is the stress tensor, p is the isotropic pressure, g_{ik} is the metric tensor of a fixed coordinate system x^i, v_i is the velocity vector. The contravariant form of e'^{ik} is given by;

$$e'^{ik} = \frac{\partial e^{ik}}{\partial t} + v^m e^{ik}_{,m} - V^k_{,m} e^{im} - v^i_{,m} e^{mk} \tag{8}$$

The convected derivative of the deformation rate tensor e^{ik} is defined by

$$2e^{ik} = v_{i,k} + v_{k,i} \tag{9}$$

Here η_0 is the limiting viscosity at the small rate of shear given by:

$$\eta_0 = \int_0^\infty N(\tau)d\tau \quad and \quad k_0 = \int_0^\infty \tau N(\tau)d\tau \tag{10}$$

$N(\tau)$ is the relaxation spectrum as discussed by (Walters, 1962). This idealized model is a valid approximation of Walters-B taking short relaxation time into account so that terms involving:

$$\int_0^\infty t^n N(\tau)d\tau \quad , n \geq 2 \tag{11}$$

has been neglected and k is taking to be significant.

Under the assumptions above, the flow equations along with the boundary constraints are:

$$\frac{\partial v^*}{\partial y^*} = 0 \tag{12}$$

$$\frac{\partial u^*}{\partial t^*} + v^* \frac{\partial u^*}{\partial y^*} = \begin{bmatrix} \nu\left(1+\frac{1}{\beta}\right)\frac{\partial^2 u^*}{\partial y^{*2}} + \sqrt{2}\nu\Gamma\frac{\partial u^*}{\partial y^*}\frac{\partial^2 u^*}{\partial y^{*2}} - \frac{\sigma B_0^2}{\rho}u^* - \frac{\nu}{K}u^* \\ -\frac{k}{\rho}\left(\frac{\partial^3 u^*}{\partial t \partial y^2} + v^*\frac{\partial^3 u}{\partial y^3}\right) \end{bmatrix} \tag{13}$$

$$\frac{\partial T}{\partial t^*}+v^*\frac{\partial T}{\partial y^*}=\alpha\frac{\partial^2 T}{\partial y^{*2}}+\frac{\nu}{c_p}\left(\frac{\partial u^*}{\partial y^*}\right)^2-\frac{1}{\rho c_p}\frac{\partial q_r}{\partial y^*}+\frac{Q_0}{\rho c_p}(T-T_\infty) \tag{14}$$

$$\frac{\partial C}{\partial t^*}+v^*\frac{\partial C}{\partial y^*}=D\frac{\partial^2 C}{\partial y^{*2}}-K_r(C-C_\infty) \tag{15}$$

subject to the constraints:

$$u=U_0, T=T_w+\psi(T_w-T_\infty)e^{n^*t^*}, C=C_w+\psi(C_w-C_\infty)e^{n^*t^*},\ at\ \ y^*=0 \tag{16}$$

$$u^*\to 0, T\to T_\infty, C\to C_\infty,\ as\ \ y^*\to\infty \tag{17}$$

By integrating the continuity equation, the suction velocity perpendicular to the plate is obtained (1). Thus, using this method, the wall suction velocity can be calculated as a function of time and a constant as follows:

$$v^*=-v_0(1+\grave{o}Ae^{n^*t^*}) \tag{18}$$

The radiation term in the energy equation is obtained by simplifying T^4 in Taylor's approach in T_∞ and forgone terms of higher order to obtain:

$$T^4\approx 4T_\infty^3T-3T_\infty^4 \tag{19}$$

Utilizing Rosse and approximation, the heat flux in terms of y^* gives

$$q_r=-\frac{4\sigma_0}{3ke}\frac{\partial T^4}{\partial y^*} \tag{20}$$

ke the mean absorption coefficient and σ_0 the Stefan-Boltzmann constant is denoted here. The tangent hyperbolic liquid is considered to be optically thick liquids since the Rosseland approximation is used in this research. By linearizing the aforementioned (9) and using the energy equation's result to obtain

$$\frac{\partial T}{\partial t^*}+v^*\frac{\partial T}{\partial y^*}=\alpha\frac{\partial^2 T}{\partial y^{*2}}+\frac{\nu}{c_p}\left(\frac{\partial u^*}{\partial y^*}\right)^2+\frac{16\sigma_0T_\infty^3}{3\rho c_p ke}\frac{\partial^2 T}{\partial y^{*2}}+\frac{Q_0}{\rho c_p}(T-T_\infty) \tag{21}$$

To simplify the flow equations in a dimensionless form, the following quantities are introduced:

$$U=\frac{u^*}{U_0}, y=\frac{v_0^2y^*}{\nu}, t=\frac{v_0^2t^*}{\nu}, n=\frac{\nu n^*}{v_0^2}, \theta=\frac{T-T_\infty}{T_w-T_\infty}, \phi=\frac{C-C_\infty}{C_w-C_\infty} \tag{22}$$

Employing the Eq. (22) above to obtain the following equations:

$$\frac{\partial U}{\partial t} - (1 + \epsilon A e^{nt})\frac{\partial U}{\partial y} = \left(1 + \frac{1}{\beta}\right)\frac{\partial^2 U}{\partial y^2} - M^2 U - \zeta\left(\frac{\partial^3 U}{\partial t \partial y^2} - (1 + \epsilon A e^{nt})\frac{\partial^3 U}{\partial y^3}\right) - \frac{1}{K}U \tag{23}$$

$$\frac{\partial \Theta}{\partial t} - (1 + \epsilon A e^{nt})\frac{\partial \Theta}{\partial y} = \left(\frac{1+R}{Pr}\right)\frac{\partial^2 \Theta}{\partial y^2} + Ec\left(\frac{\partial U}{\partial y}\right)^2 + Q\Theta \tag{24}$$

$$\frac{\partial \Phi}{\partial t} - (1 + \epsilon A e^{nt})\frac{\partial \Phi}{\partial y} = \frac{1}{Sc}\frac{\partial^2 \Phi}{\partial y^2} - Kr\Phi \tag{25}$$

Subject to:

$$U = 1,\ \Theta = 1 + \epsilon e^{nt},\ \Phi = 1 + \epsilon e^{nt},\quad at\quad y = 0 \tag{26}$$

$$U \longrightarrow 0,\ \Theta \longrightarrow 0,\ \Phi \longrightarrow 0,\quad at\quad y \longrightarrow \infty \tag{27}$$

3. Spectral Relaxation Technique (SRM)

SRM is employed in this section on the dimensionless systems of PDEs in Eq. (23) to Eq. (25) subject to Eq. (26) and Eq. (27). The SRM is an iterative technique which uses the concept of Gauss-Siedel technique to decouple and linearize the transformed nonlinear and coupled PDEs. This technique (SRM) is credited to Motsa (2014). After using the Gauss-Siedel technique, the Chebyshev pseudo-spectral method is further used to discretize and solve the set of PDEs. The linear terms are denoted by $r + 1$ at the current iteration while r at the previous iteration. Using SRM on the Eq. (23) to (25) subject to Eq. (26) and Eq. (27) to obtain:

$$\frac{\partial U_{r+1}}{\partial t} + \frac{\partial^3 U_{r+1}}{\partial t \partial y^2} = \left(1 + \frac{1}{\beta}\right)\frac{\partial^2 U_{r+1}}{\partial y^2} + a_{0,r}\frac{\partial U_{r+1}}{\partial y} + a_{1,r}\frac{\partial^2 U_{r+1}}{\partial y^2} - M^2 U_{r+1} + a_{0,r}\frac{\partial^3 U_{r+1}}{\partial y^3} + a_{2,r} + \frac{1}{Po}U_{r+1} \tag{28}$$

$$\frac{\partial \Theta_{r+1}}{\partial t} = b_{0,r}\frac{\partial^2 \Theta_{r+1}}{\partial y^2} + a_{0,r}\frac{\partial \Theta_{r+1}}{\partial y} + b_{1,r} + Q\Theta_{r+1} + b_{2,r} \tag{29}$$

$$\frac{\partial \Phi_{r+1}}{\partial t} = \frac{1}{Sc}\frac{\partial^2 \Phi}{\partial y^2} + a_{0,r}\frac{\partial \Phi}{\partial y} - Kr\Phi_{r+1} \tag{30}$$

Subject to:

$$U_{r+1}(0,t) = 1,\ U_{r+1}(\infty,t) = 0,\ \Theta_{r+1}(0,t) = 1 + \epsilon e^{nt} \tag{31}$$

$$\Theta_{r+1}(\infty,t) = 0,\ \Phi_{r+1}(0,t) = 1 + \epsilon e^{nt},\ \Phi_{r+1}(0,t) = 0 \tag{32}$$

Where coefficient parameters are defined as follows:

$$a_{0,r} = (1 + \epsilon A e^{nt}),\ a_{1,r} = \alpha n\frac{\partial U_{r+1}}{\partial y},\ a_{2,r} = Gr\Theta_r + Gm\Phi_r,\ b_{0,r} = \left(\frac{1+R}{Pr}\right)$$

$$b_{1,r} = Ec\left(\frac{\partial U_{r+1}}{\partial y}\right)^2,\quad b_{2,r} = M^2 Ec U_{r+1}^2$$

The starting guess is chosen to satisfy the boundary constraints (26) and (27). These guesses are defined as follows:

$$e^{-y} = U_0,\ \Theta_0 - \epsilon e^{nt} = e^{-y},\ \Phi_0 - \epsilon e^{nt} = e^{-y} \tag{33}$$

The equation defined in Eq. (28) to Eq. (30) above are solved iteratively where $r = 0,1,2$. These equations were solved with the help of Gauss-Lobatto collocation point defined as [37]:

$$\xi_j = \cos(\pi j)(N)^{-1},\quad j = 0,1,2,\dots,N,\quad 1 \le \xi \le -1 \tag{34}$$

Where N is the collocation point. To employ the Eq. (34) above, the physical domain $[0,\infty]$ of the model is transformed to $[-1,1]$.

4. Results and Discussion

Using In this section, an illustration of graphical outcomes for the dimensionless temperature $\Theta(t,y)$, velocity $\mathrm{U}(t,y)$ and concentration $\Phi(t,y)$ for various flow parameters are presented from Figure 2 to Figure 8. The impact of flow parameters on the local Sherwood number, local skin friction and local Nusselt number are computed and tabulated.

Figure 2 shows the effect of the magnetic parameter (M) on the velocity distribution. An increase in M is observed to decrease the velocity as well as the hydrodynamic boundary layer thickness. The magnetic field strength gives rise to the Lorentz force which is capable of slowing down the motion of electrically conducting fluids. Figure 3 shows the effect of the permeability parameter (K) on the velocity distributions. An increase in the value of K is observed to elevate the velocity distribution. Physically, the porosity parameter allows the passage of fluid particles within the boundary layer. Therefore, increasing the intensity of this parameter enhances the hydrodynamic boundary layer.

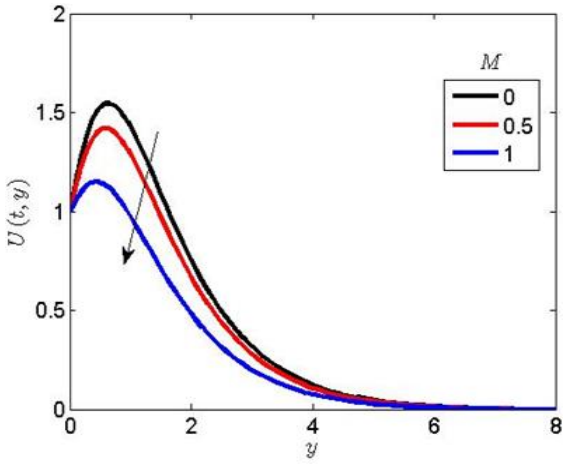

Fig. 2 Effect magnetic parameter (M) on the velocity distribution

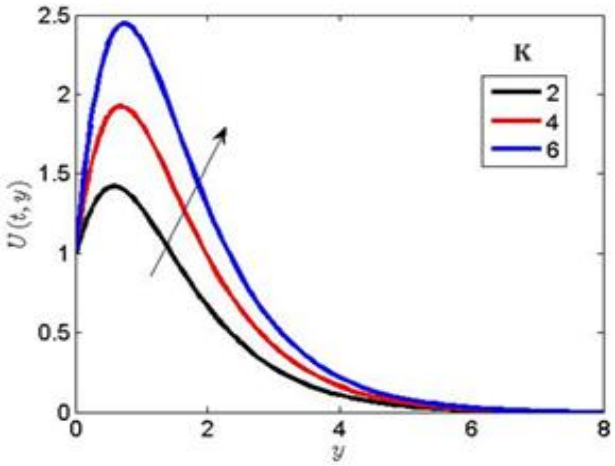

Fig. 3. Effect porosity parameter (K) on the velocity distribution

Figure 4 represents the effect of Prandtl number (Pr) on the temperature and velocity distributions respectively. An increase in the value of Pr is noticeable to lessen the velocity and temperature distributions. Physically, an increase in Pr leads to decrease in thermal diffusivity and hereby decrease the heat transfer ability within the thermal boundary layer. In the phenomena of

heat transfer, any fluid with higher Pr obtains greater viscosities which serves to reduce velocities and lower the local skin friction. It should be noted that, if Pr is small (i.e. Pr<1).

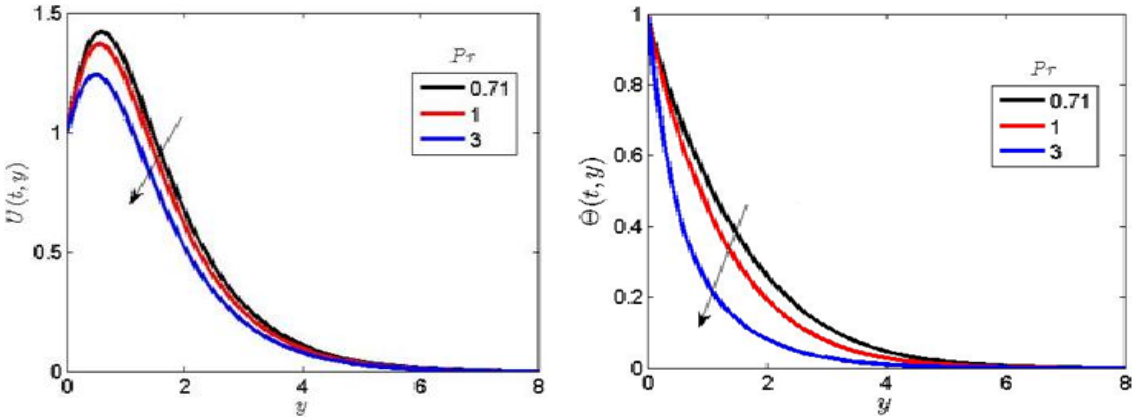

Fig. 4. Effect of Prandtl number on velocity and temperature distributions

Figure 5 illustrates the effect of thermal radiation (R) on the temperature and velocity distributions respectively. An increase in R is observed to enhance the temperature as well as velocity distributions. Physically, the presence of radiation in heat transfer process enhances the intensity of temperature within the boundary layer. Thermal radiation enhances convective flow starting from the wall to the free stream. However, an increase in R produces an increase in thermal condition of the fluid and the thermal boundary layer.

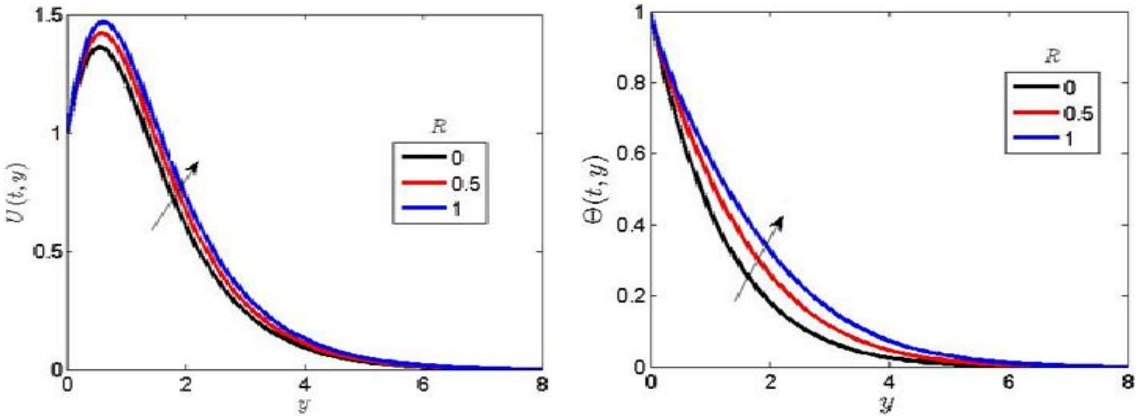

Fig. 5. Effect of thermal radiation on the velocity and temperature distributions

Figure 6 represents the effect of chemical reaction parameter (Kr) on the velocity and concentration distributions. A higher value of the chemical reaction parameter (Kr) degenerates the velocity and concentration distributions. Physically, as Kr increases the molecular liquid becomes very weak such that the fluid species is affected and a decrease in the specie boundary layer is observed.

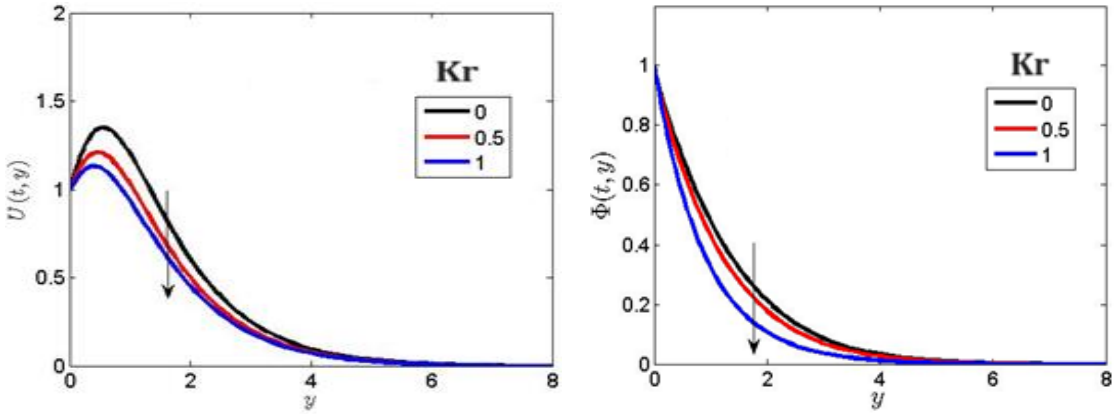

Fig. 6. Effect of chemical reaction parameter on the velocity and concentration distributions

Figure 7 depicts the effect of Eckert number (Ec) on the velocity and temperature distributions. An increase in Ec is observed to enhance velocity and temperature distributions respectively. Ec is the relationship between kinetic energy and enthalpy. Hence, as enthalpy increases, the temperature distribution increases due to the presence of thermal radiation parameter. Higher viscous dissipative heat leads to enhancement in velocity and temperature.

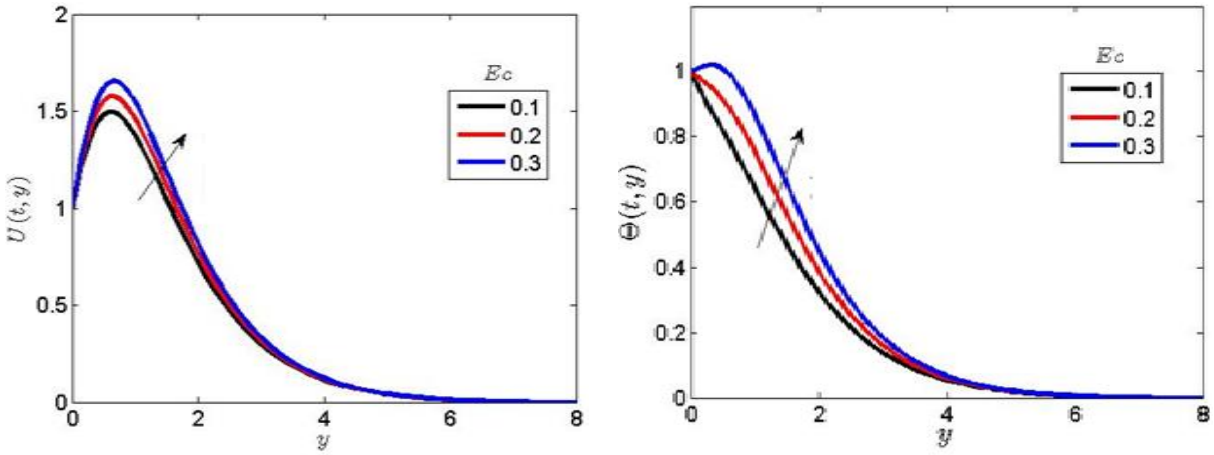

Fig. 7. Effect of Eckert number on the velocity and temperature distributions

Figure 8 illustrates the effect of Schmidt number (Sc) on the velocity and concentration distributions. Schmidt number plays a significant role in the mass transfer process. When Sc=0, it shows the absence of mass transport and mass buoyancy effects. From Figure 8, there is degeneration in the velocity and concentration distributions due to an increase in Sc. Hence, a decrease in the hydrodynamic and solutal boundary layer is observed as a result of an increase in Sc.

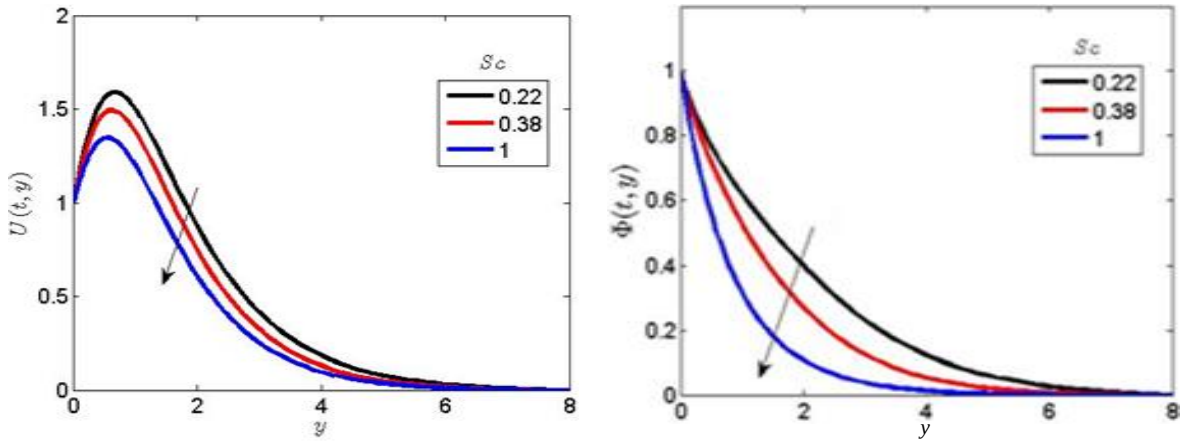

Fig. 8. Effect of Schmidt number on the velocity and concentration distributions

The values of engineering relevance, including local skin friction, local Nusselt number, and local Sherwood number, are shown in Table 1 as a function of the flow parameters Pr, R, Ec, Kr, Sc, K, and M. The rate of mass movement and local skin friction are seen to decrease when Sc and Kr values increase. It is noted that a larger value of Pr lowers the skin friction coefficient and accelerates the rate of mass movement. By reducing the hydrodynamic boundary layer, a greater value of the magnetic parameter is seen to strengthen the Lorentz force. It is noticed that a greater Eckert number and thermal radiation parameter value accelerate the pace of heat transfer.

Table 1
Computational values of pertinent flow parameters on the local skin friction U(0), local Nusselt number $\theta(0)$ and local Sherwood number $\phi(0)$

Pr	R	Ec	Kr	Sc	K	M	U(0)	$\theta(0)$	$\phi(0)$
0.71							1.4328	0.6935	0.7633
1.0							1.3073	0.8038	0.7633
3.0							0.9461	1.5919	0.7633
	0.0						1.2847	0.8291	0.5271
	0.5						1.4328	0.6935	0.5271
	1.0						1.5399	0.6299	0.5271
		0.1					1.6306	0.4365	0.7968
		0.2					1.8285	0.1793	0.7968
		0.3					2.0264	-0.0778	0.7968
			0.0				1.5069	0.8299	0.7655
			0.5				1.4328	0.8299	0.8633
			1.0				1.2533	0.6935	1.0904
				0.22			1.8171	0.3918	0.6223
				0.38			1.6072	0.3918	0.7169
				1.0			1.2463	0.3918	1.1372
					0.2		1.4328	0.9918	0.5171
					0.4		2.7985	0.9918	0.5171
					0.6		4.1643	0.9918	0.5171

5. Conclusion

This study examined the dynamics of tangent hyperbolic and Walters-B non-Newtonian fluids flow under the contribution of thermal radiation. The analysis is basically on constant viscosity and thermal conductivity. The transformed model equations were solved numerically by utilizing the SRM. From the results obtained, the following findings were noted:

i. The imposed magnetic field is noted to slow down the motion of both tangent hyperbolic and viscoelastic liquids due to the Lorentz force.
ii. A higher value of the Prandtl number is observed to decline the hydrodynamic and thermal boundary layer by decreasing the fluid velocity and temperature.
iii. Increase in the value of Schmidt and chemical reaction parameter is noticed to decelerate the velocity and concentration distributions.
iv. A higher value of the thermal radiation parameter is observed to enhance the thermal condition and thermal layer of the fluid.

References

[1] Hayat, T., M. Ijaz Khan, M. Farooq, A. Alsaedi, M. Waqas, and Tabassam Yasmeen. "Impact of Cattaneo-Christov heat flux model in flow of variable thermal conductivity fluid over a variable thicked surface." *International Journal of Heat and Mass Transfer* 99 (2016): 702-710. https://doi.org/10.1016/j.ijheatmasstransfer.2016.04.016
[2] Khan, Umar, Naveed Ahmed, and Syed Tauseef Mohyud-Din. "Thermo-diffusion and diffusion-thermo effects on flow of second grade fluid between two inclined plane walls." *Journal of Molecular Liquids* 224 (2016): 1074-1082. https://doi.org/10.1016/j.molliq.2016.10.068
[3] Khan, Muhammad Ijaz, Muhammad Waqas, Tasawar Hayat, and Ahmed Alsaedi. "A comparative study of Casson fluid with homogeneous-heterogeneous reactions." *Journal of Colloid and Interface Science* 498 (2017): 85-90. https://doi.org/10.1016/j.jcis.2017.03.024
[4] Adnan, Adnan,Syed Zulfiqar Ali Zaidi, Umar Khan, Naveed Ahmed, Syed Tauseef Mohyud-Din, Yu-Ming Chu, Ilyas Khan, and Kottakkaran Sooppy Nisar. "Impacts of freezing temperature based thermal conductivity on the heat transfer gradient in nanofluids: applications for a curved Riga surface." *Molecules* 25, no. 9 (2020): 2152. https://doi.org/10.3390/molecules25092152
[5] Neffah, Z., H. Kahalerras, and B. Fersadou. "Heat and mass transfer of a non-newtonian fluid flow in an anisotropic porous channel with chemical surface reaction." *Fluid Dynamics & Materials Processing* 14, no. 1 (2018): 39-56.
[6] Eberhard, Ursin, Hansjoerg J. Seybold, Marius Floriancic, Pascal Bertsch, Joaquin Jiménez-Martínez, José S. Andrade Jr, and Markus Holzner. "Determination of the effective viscosity of non-Newtonian fluids flowing through porous media." *Frontiers in Physics* 7 (2019): 71. https://doi.org/10.3389/fphy.2019.00071
[7] Gomez-Constante, Juan P., and Kumbakonam R. Rajagopal. "Flow of a new class of non-Newtonian fluids in tubes of non-circular cross-sections." *Philosophical Transactions of the Royal Society A* 377, no. 2144 (2019): 20180069. https://doi.org/10.1098/rsta.2018.0069
[8] Ionescu, Clara-Mihaela, Isabela Roxana Birs, Dana Copot, C. I. Muresan, and R. Caponetto. "Mathematical modelling with experimental validation of viscoelastic properties in non-Newtonian fluids." *Philosophical Transactions of the Royal Society A* 378, no. 2172 (2020): 20190284. https://doi.org/10.1098/rsta.2019.0284
[9] Seybold, H. J., U. Eberhard, Eleonora Secchi, Roberto L. C. Cisne Jr, Joaquin Jiménez-Martínez, Roberto F. S. Andrade, A. D. Araújo, Markus Holzner, and José S. Andrade Jr. "Localization in flow of non-Newtonian fluids through disordered porous media." *Frontiers in Physics* 9 (2021): 635051. https://doi.org/10.3389/fphy.2021.635051
[10] de Goede, Thijs C., Karla G. de Bruin, and Daniel Bonn. "High-velocity impact of solid objects on Non-Newtonian Fluids." *Scientific Reports* 9, no. 1 (2019): 1250. https://doi.org/10.1038/s41598-018-37543-1
[11] Tao, Chengcheng, Wei-Tao Wu, and Mehrdad Massoudi. "Natural convection in a non-Newtonian fluid: Effects of particle concentration." *Fluids* 4, no. 4 (2019): 192. https://doi.org/10.3390/fluids4040192
[12] Reddy, K. Veera, G. Venkata Ramana Reddy, and Ali J. Chamkha. "Effects of viscous dissipation and thermal radiation on an electrically conducting Casson-Carreau nanofluids flow with Cattaneo-Christov heat flux model." *Journal of Nanofluids* 11, no. 2 (2022): 214-226. https://doi.org/10.1166/jon.2022.1836
[13] Hayat, Tasawar, Anum Shafiq, Meraj Mustafa, and Ahmed Alsaedi. "Boundary-layer flow of Walters' B fluid with Newtonian heating." *Zeitschrift für Naturforschung A* 70, no. 5 (2015): 333-341. https://doi.org/10.1515/zna-2014-0280
[14] Reddy, C. Srinivas, B. Mahanthesh, P. Rana, and K. S. Nisar. "Entropy generation analysis of tangent hyperbolic fluid in quadratic Boussinesq approximation using spectral quasi-linearization method." *Applied Mathematics and Mechanics* 42 (2021): 1525-1542. https://doi.org/10.1007/s10483-021-2773-8
[15] Hussain, Azad, and Anwar Ullah. "Boundary layer flow of a Walter's B fluid due to a stretching cylinder with temperature dependent viscosity." *Alexandria Engineering Journal* 55, no. 4 (2016): 3073-3080. https://doi.org/10.1016/j.aej.2016.07.037

[16] Tonekaboni, Seyed Ali Madani, Ramin Abkar, and Reza Khoeilar. "On the study of viscoelastic Walters' B fluid in boundary layer flows." *Mathematical Problems in Engineering* 2012 (2012). https://doi.org/10.1155/2012/861508
[17] Awasthi, Mukesh Kumar, Dharamendra, and Dhananjay Yadav. "Stability characteristics of Walter's B viscoelastic fluid in a cylindrical configuration with heat transfer." *Proceedings of the Institution of Mechanical Engineers, Part C: Journal of Mechanical Engineering Science* 236, no. 19 (2022): 10370-10377. https://doi.org/10.1177/09544062221101831
[18] Hussain, Arif, M. Y. Malik, T. Salahuddin, A. Rubab, and Mair Khan. "Effects of viscous dissipation on MHD tangent hyperbolic fluid over a nonlinear stretching sheet with convective boundary conditions." *Results in Physics* 7 (2017): 3502-3509. https://doi.org/10.1016/j.rinp.2017.08.026
[19] Ali, A., R. Hussain, and Misbah Maroof. "Inclined hydromagnetic impact on tangent hyperbolic fluid flow over a vertical stretched sheet." *AIP Advances* 9, no. 12 (2019). https://doi.org/10.1063/1.5123188
[20] Ibrahim, Wubshet. "Magnetohydrodynamics (MHD) flow of a tangent hyperbolic fluid with nanoparticles past a stretching sheet with second order slip and convective boundary condition." *Results in Physics* 7 (2017): 3723-3731. https://doi.org/10.1016/j.rinp.2017.09.041
[21] Usman, Muhammad, Tamour Zubair, Muhammad Hamid, Rizwan Ul Haq, and Zafar Hayat Khan. "Unsteady flow and heat transfer of tangent-hyperbolic fluid: Legendre wavelet-based analysis." *Heat Transfer* 50, no. 4 (2021): 3079-3093. https://doi.org/10.1002/htj.22019
[22] Chu, Yu-Ming, Mujeeb ur Rahman, M. Ijaz Khan, Seifedine Kadry, Wasif Ur Rehman, and Zahra Abdelmalek. "Heat transport and bio-convective nanomaterial flow of Walter's-B fluid containing gyrotactic microorganisms." *Ain Shams Engineering Journal* 12, no. 3 (2021): 3071-3079. https://doi.org/10.1016/j.asej.2020.10.025
[23] Hayat, T., Sadia Asad, M. Mustafa, and Hamed H. Alsulami. "Heat transfer analysis in the flow of Walters' B fluid with a convective boundary condition." *Chinese Physics B* 23, no. 8 (2014): 084701. https://doi.org/10.1088/1674-1056/23/8/084701
[24] Asjad, Muhammad Imran, Maryam Aleem, and M. Bilal Riaz. "Exact analysis of MHD Walters-B fluid flow with non-singular fractional derivatives of Caputo-Fabrizio in the presence of radiation and chemical reaction." *Journal of Polymer Science and Engineering* 1 (2018): 599. https://doi.org/10.24294/jpse.v1i2.599
[25] Salahuddin, T., Moeen Taj, K. Ayoub, and Mair Khan. "Effect of Coriolis and buoyancy forces on three-dimensional flow of chemically reactive tangent hyperbolic fluid subject to variable viscosity." *Arabian Journal of Chemistry* 16, no. 3 (2023): 104446. https://doi.org/10.1016/j.arabjc.2022.104446
[26] Salahuddin, T., M. Y. Malik, Arif Hussain, Muhammad Awais, Imad Khan, and Mair Khan. "Analysis of tangent hyperbolic nanofluid impinging on a stretching cylinder near the stagnation point." *Results in Physics* 7 (2017): 426-434. https://doi.org/10.1016/j.rinp.2016.12.033
[27] Dharmaiah, G., B. Shankar Goud, Nehad Ali Shah, and Muhammad Faisal. "Numerical analysis of heat and mass transfer with viscous dissipation, Joule dissipation, and activation energy." *International Journal of Ambient Energy* (2023): 1-13. https://doi.org/10.1080/01430750.2023.2224335
[28] Kumar, T. Prasanna, G. Dharmaiah, Khaled AL-Farhany, Mohammed Azeez Alomari, Mujtaba A. Flayyih, Wasim Jamshed, and Siti Suzilliana Putri Mohamed Isa. "Perturbation methodology for electromagnetic radiative fluxing of chemical reactive Casson fluid flow under heat source (sink) effectiveness." *International Journal of Modern Physics B* (2023): 2350243. https://doi.org/10.1142/S0217979223502430
[29] Rani, K. Sandhya, G. Venkata Ramana Reddy, and Abayomi Samuel Oke. "Significance of Cattaneo-Christov Heat Flux on Chemically Reacting Nanofluids Flow Past a Stretching Sheet with Joule Heating Effect." *CFD Letters* 15, no. 7 (2023): 31-41. https://doi.org/10.37934/cfdl.15.7.3141
[30] Vyakaranam, Seethamahalakshmi, Rekapalli Leelavathi, Tagallamudi Srinivasa Rao, Venkata Ramana Reddy Gurrampati, and Oke Abayomi Samuel. "Soret-Dufour Mechanisms on Unsteady Boundary Layer Flow of Tangent Hyperbolic and Walters-B Nanoliquid." *Journal of Advanced Research in Fluid Mechanics and Thermal Sciences* 108, no. 1 (2023): 13-27. https://doi.org/10.37934/arfmts.108.1.1327
[31] Rani, K. Sandhya, and Venkata Ramana Reddy Gurrampati. "Cattaneo-Christov Heat and Mass Transfer Flux Across Electro-Hydrodynamics Blood-Based Hybrid NanoFluid Subject to Lorentz Force." *CFD Letters* 14, no. 7 (2022): 124-134. https://doi.org/10.37934/cfdl.14.7.124134
[32] Suneetha, K., S. M. Ibrahim, and G. V. Ramana Reddy. "Radiation and heat source effects on MHD flow over a permeable stretching sheet through porous stratum with chemical reaction." *Multidiscipline Modeling in Materials and Structures* 14, no. 5 (2018): 1101-1114. https://doi.org/10.1108/MMMS-12-2017-0159
[33] Reddy, G. V. R., and Y. Hari Krishna. "Soret and dufour effects on MHD micropolar fluid flow over a linearly stretching sheet, through a non-darcy porous medium." *International Journal of Applied Mechanics and Engineering* 23, no. 2 (2018): 485-502. https://doi.org/10.2478/ijame-2018-0028

[34] Nagasantoshi, P., G. V. Reddy, M. Gnaneswara Reddy, and P. Padma. "Heat and mass transfer of Non-Newtonian Nanofluid flow over a stretching sheet with non-uniform heat source and Variable viscosity." *Journal of Nanofluids* 7, no. 5 (2018): 821-832. https://doi.org/10.1166/jon.2018.1517

[35] Lakshmi, R., K. R. Jayarami, K. Ramakrishna, and G. V. Ramana Reddy. "Numerical Solution of MHD flow over a moving vertical porous plate with heat and Mass Transfer." *International Journal of Chemical Sciences* 12, no. 4 (2014): 1487-1499.

[36] Vyakaranam, Seethamahalakshmi, Bindu Pathuri, Venkata Ramana Reddy Gurrampati, and Abayomi Samuel Oke. "Flow of Casson Nanofluid Past a Permeable Surface: Effects of Brownian Motion, Thermophoretic Diffusion and Lorenz force." *CFD Letters* 14, no. 12 (2022): 111-125. https://doi.org/10.37934/cfdl.14.12.111125

[37] Reddy, G. Venkata Ramana, Ali Akgül, and Muhammad Bilal Riaz. "Unsteady mhd flow of tangent hyperbolic liquid past a vertical porous plate plate." *Heliyon* 9, no. 8 (2023). https://doi.org/10.1016/j.heliyon.2023.e18478